A Design-of-Experiments Approach to Characterizing Beam-Induced Deposition in the Helium Ion Microscope

Larry Scipioni,[1] * Colin Sanford,[1] Emile van Veldhoven,[2] and Diederik Maas[2]
[1]Carl Zeiss NTS, LLC, 1 Corporation Way, Peabody, MA 01960, USA
[2]TNO Science and Industry—Van Leeuwenhoek Laboratory, P.O. Box 155, 2600AD Delft, The Netherlands
* l.scipioni@nts.zeiss.com

Introduction

Charged particle microscopes have been used extensively for the creation of nanostructures. As a subset of the techniques for this, the process of beam-induced chemistry offers almost endless flexibility for both additive (by beam-driven precursor deposition) and subtractive (by beam-catalyzed etching) processing. A recent review article [1] makes it evident simply by its massive page count the number of materials that have been used to deposit a variety of conductive, insulating, magnetic, photonic, and other structures. To take advantage of these capabilities, though, the nanoarchitect must select the correct settings for a large number of parameters. One key figure of interest is the size of features that can be written by deposition of conducting material: how small can we go? Process development is complex, however: a standard beam-induced deposition process using the system described below calls for the control of sixteen different parameters! Several of these are used to set the flow of the reactant, several are required for defining the particle beam, and yet another set of parameters call out the routine by which the beam is scanned over the pattern of interest. In the end, the result provides just one recipe for one chemistry with one beam type. The wide scatter of reported outcomes in the review article mentioned above indicates the complexity of the problem, where each result given can be considered just a snapshot of one small corner of the parameter space. Our goal here is to apply a quantitative optimization methodology for the determination of beam chemistry processes in the helium ion microscope (HIM). In this article, we discuss efforts toward finding the minimum obtainable line width and gap width between line pairs of deposited platinum lines and giving a predictive formulation of the same.

The HIM, first commercially available in 2007 [2], has demonstrated imaging resolution better than 0.35 nm. The small size of the probe, combined with the light mass of the ion and the specific beam-sample interactions, have also inspired experiments in nanofabrication. For example, milling [3] of 5-nm holes of high aspect ratio in a variety of materials has been demonstrated. Small, dense features have also been created with lithography and beam-induced deposition [4]. Over the past year, Carl Zeiss NTS, LLC (Peabody, MA) and TNO (Delft, The Netherlands) have been jointly pursuing characterization of beam-induced chemistry processes in HIM. There are several features of these processes to characterize: deposition size, deposition rate, chemical purity of deposits, and the electrical resistivity of deposits (both conductors and insulators). Most of this work to date has concentrated on the characterization of deposited conducting features from a common platinum precursor. The processes have to be recharacterized for each different performance dimension desired; for example, the smallest features might not also have the lowest resistivity. One quickly realizes that there is a large manifold of parameters to search over for these optima. A design-of-experiments (DOE) approach allows us to vary parameters thought to be most important for determining feature performance and then to cast quantitative relations between these process settings and the outcomes. This approach is explained in more detail in the next sections.

Materials and Methods

All sample creation and inspection was carried out in an Orion Plus® HIM (Carl Zeiss NTS, LLC) located at TNO Science and Industry in Delft, The Netherlands. The tool was equipped with an OmniGIS (OmniProbe) gas injection system. This device houses reservoirs for three different reactive gases and has inputs for two carrier gases, to vary the flow and concentration of the active species. For all of the experiments reported here, deposition of platinum (bearing) deposits were generated from MeCpPt(IV)Me_3 precursor (Colonial Metals). The precursor was kept at a constant temperature of 30°C. The needle of the gas injection was placed at a distance of 100 mm from the target area. The gas flow was kept constant to give a steady chamber pressure of 4×10^{-6} Torr. For maximum flexibility in defining writing strategies, the scan during deposition was controlled by an Elphy Plus (Raith GmbH) lithography pattern generator. A set of two lines with various pitches (48, 28, 24, 20, 16, 12, and 8 nm) was taken as the design. The experiments were generated with the DOE approach. DOE PRO XL software (Sigmazone.com), which runs as an extension to Microsoft Excel, was used for experimental setup and analysis of results. Four factors were initially considered as having influence on the width of the lines: primary ion beam current, ion beam dwell time per point, pixel step size per point, and writing direction (that is, lines oriented perpendicular to or parallel to beam scanning direction). A four-dimensional experiment would be quite extensive, so two of these parameters were fixed, based on existing experimental evidence. Previous work on pillar growth [5] showed that the narrowest and tallest pillars are obtained when the beam current is kept below 0.8 pA, so a primary beam current of 0.5 pA was used for the experiments herein. The beam energy was 25 keV. Second, preliminary experiments determined that writing perpendicular to the line orientation provides consistently narrower lines. Thus only two parameters were chosen to be varied: step size and dwell time. The parameter space was setup for a dwell time between 0.2 and 19.8 µs and a step

https://doi.org/10.1017/S1551929511000307 Published online by Cambridge University Press

Unmatched Microscopy for Life Science Applications

Shuttle & Find

Bridging the Micro and Nano World

Discover new dimensions of information by effectively combining Light and Electron microscopes with Shuttle & Find for Life Sciences

- Correlate functional and structural information
- Zoom in from micro to nano
- Overlay LM and EM images to generate a new level of information

ATLAS™

Large Area Imaging for Unrivaled Productivity

- Highly automated, multi-site image acquisition
- Built-in tiling mechanism
- Freely configurable image sizes up to 32 k x 32 k
- Full flexibility in choice of detectors

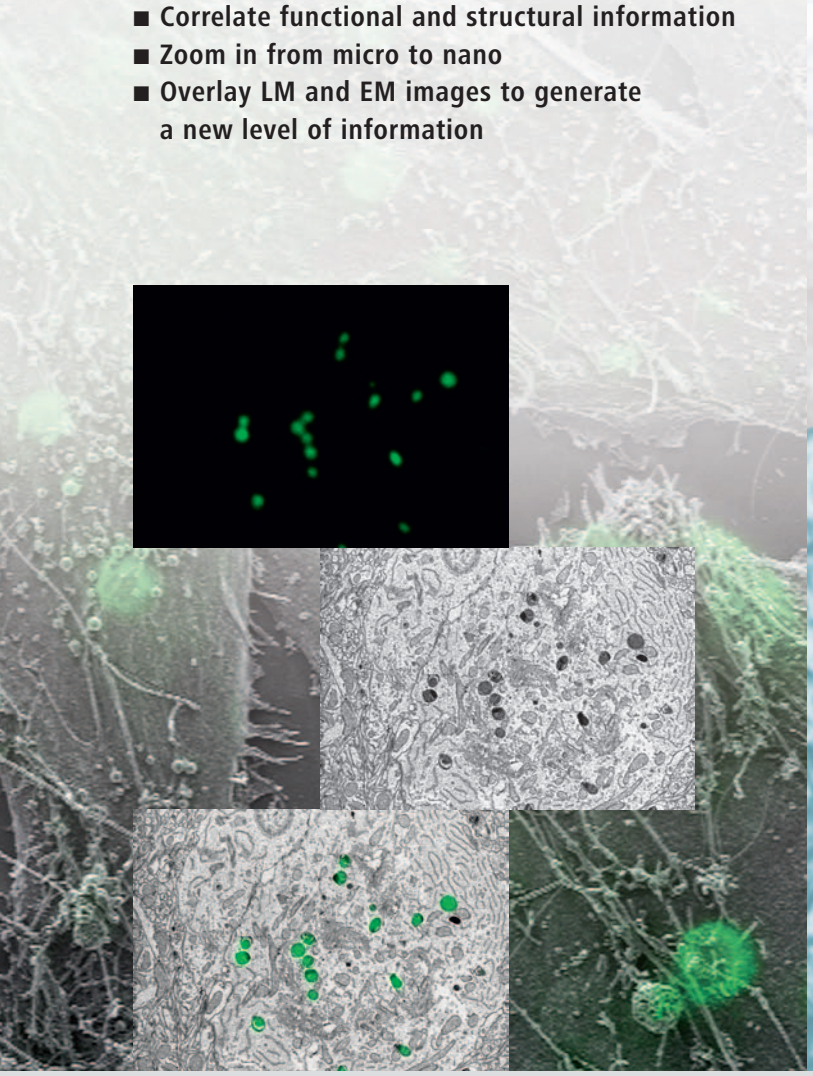

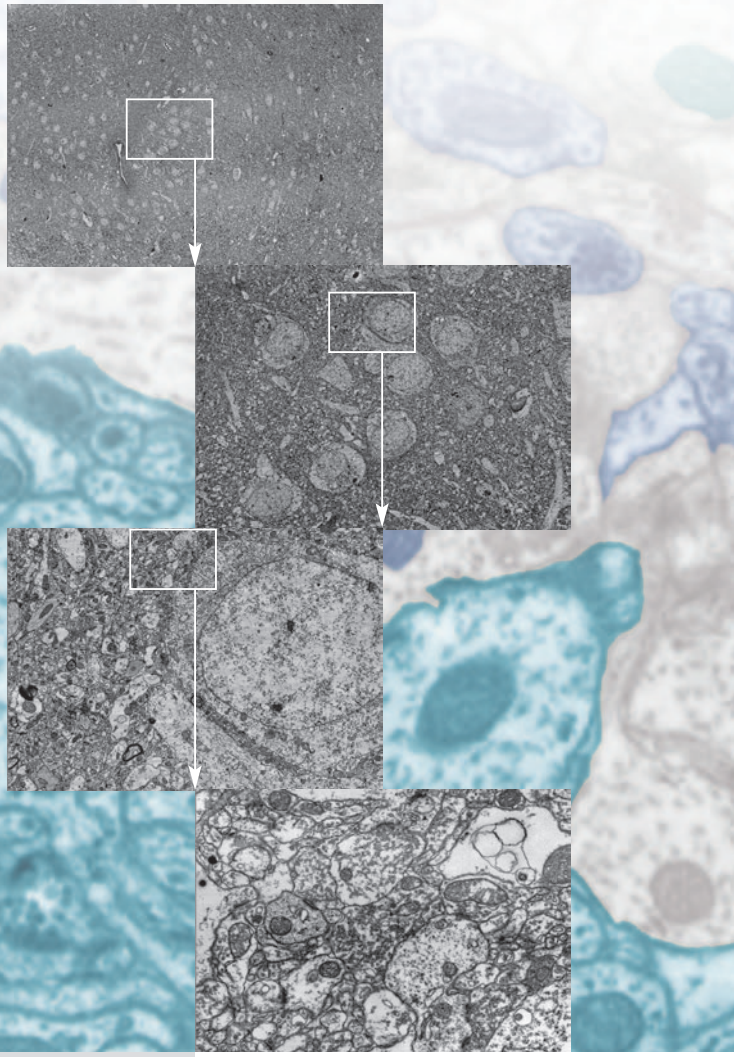

For information about Light Microscopes please contact:

Carl Zeiss MicroImaging, LLC
One Zeiss Drive, Thornwood, New York 10594
Tel. 1-800-233-2343, micro@zeiss.com
www.zeiss.com/micro

For information about Electron and Ion Beam Microscopes please contact:

Carl Zeiss NTS, LLC
One Corporation Way, Peabody, MA 01960,
Tel. 1-978-826-1500, info-usa@nts.zeiss.com
www.zeiss.com/nts

ZEISS

We make it visible.

size between 1 and 4 nm. In each case the total line dose was held fixed (at 4.8 nC/cm) by adjusting the number of writing repeats of the pattern. Center points are included in the design to allow modeling of non-linear behavior. The step size center point was set to 2 nm (rather than 2.5 nm) to avoid aliasing artifacts. This DOE generated the set of 10 experiments listed in Table 1. A Si wafer was taken as substrate to perform the experiments.

Results

Table 1 shows the 10 parameter combinations that were executed in the experiment. Because we looked at 7 different pitches (defined as the programmed spacing between the line pairs) in our line pairs, a total of 70 experiments were carried out. Figure 1 shows as an example result from experiment 2, for 6 of the 7 line pairs. Not shown is the smallest (8 nm) pitch, where the two lines were obviously melded into one; these data were not fully processed. The selected range of the pitch evidently covers the transition from isolated to merged lines.

The line width can now be expressed as a function of the parameters:

$$W(nm) = C + A\cdot(step\ size) + B\cdot(dwell\ time) + AB\cdot(step\ size)\cdot(dwell\ time) + AA\cdot(step\ size)^2 + BB\cdot(dwell\ time)^2 \quad (1)$$

where W is line width (nm), C is a constant, A is a prefactor for step size, B is a prefactor for dwell time, AB is a prefactor for step size times dwell time, AA is a prefactor for step size squared, and BB is a prefactor for dwell time squared.

Line-width measurements were made from HIM images. Line scans were taken in four places for each line pair. Each profile scan is actually an average of 17 adjacent rows of pixels, corresponding to a 24.9-nm distance along the lines. The edge position was determined manually as the position at which the gray value was halfway between the peak and the baseline. See Figure 2 for an example. It was found in the measurements that the image gray level did not return to the base line for the 12-nm pitch lines, from which we conclude that these lines were not fully separated when written. The analysis was thus ended at the 16-nm pitch. Figure 3 shows a survey of all the results with line width plotted as a function of pitch for all ten parameter sets. The reader can promptly observe that experiment 2 consistently provided the narrowest lines. Although the factor analysis has been carried out for all the experiments, we will show just some illustrative examples here.

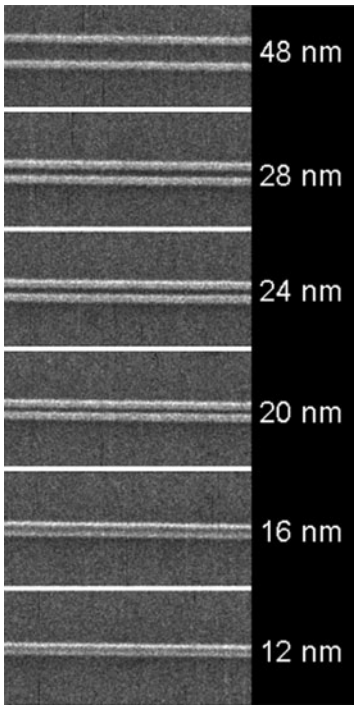

Figure 1: Pairs of Pt lines from experiment 2. Writing was carried out in each case in a 10-μm field of view, with a raster perpendicular to the line direction. The programmed pitch between the lines pairs, as laid out from left to right in this montage, are 48 nm, 28 nm, 24 nm, 20 nm, 16 nm, and 12 nm. The lines at 8-nm pitch overlapped and therefore are not shown.

We take as an example the 48-nm pitch line pair experiments. The values for the coefficients in Equation (1) were derived from the factor analysis, and a confidence level in their significance was calculated. A numerical figure of merit, P, should generally be below 0.05. The reader is referred to Reference [6] for a definition of this metric. The positive value of A obtained (0.70) indicates that increasing step size increases line width, whereas the negative value of B (–1.58) shows that a larger dwell time is favorable for decreasing line width. This is also observed graphically by the Marginal Means plots in Figure 4. We note in this experiment the value for AB (0.66) has a marginal P value of 0.02, leading to an initial conclusion that there is some level of interaction between step size and dwell time. The coefficient of determination (R^2 = 0.5907) gives an indication that the fit is somewhat low in this case; a value of 0.9 signifies high

Table 1: The 10 experimental runs carried out for each of 7 pairs of lines of different spacing in order to determine the influencers on line width.

Factor	A	B
Row #	Step Size	Dwell Time
1	1	0.2
2	1	19.8
3	4	0.2
4	4	19.8
5	2	10
6	2	10
7	1	10
8	4	10
9	2	0.2
10	2	19.8

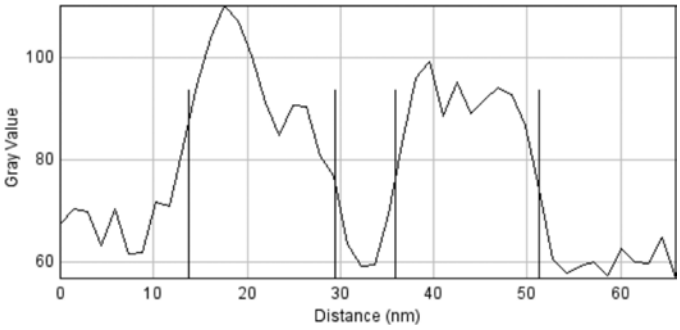

Figure 2: Example line scan (experiment 2, 20-nm pitch) used for measurement of line and gap width. Line width is measured as the full width at half maximum signal. In each of 4 positions along the lines, a scan like this was generated by averaging together 17 adjacent rows. The line and gap widths were determined using the coordinates noted where the vertical reference marks are here. The asymmetric appearance of the left line in particular is attributed to the off-axis signal collection.

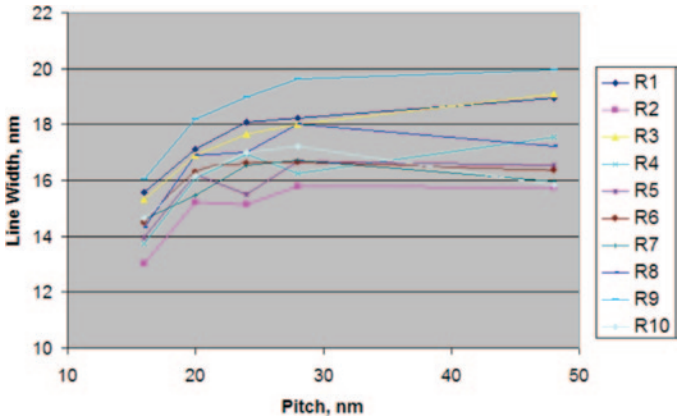

Figure 3: Plots of line width vs. pitch. The lines are a guide to the eye. The 10 trend lines correspond to the ten rows of the experiment as defined in Table 1. The line width appears to be sensitive to the pitch at the low end. Experiment #2 consistently gives the smallest line width.

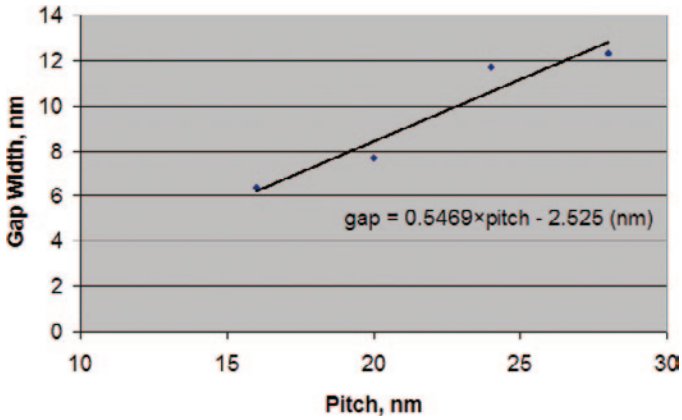

Figure 5: Plot of gap width as function of pitch for experiment 2. The 48-nm pitch result is not included in order to emphasize the trend at small pitch. The solid line is a best fit to a straight line, and the equation of that line is displayed as well.

confidence, so the inclusion of more factors into the model should be considered. We will touch on these fit issues in the discussion below. Finally, the multiple response prediction gives us a 99-percent confidence level that the significant constant $C = 16 \pm 3$ nm, 3 s.

Figure 4 contains factor analysis plots that can display trends and interactions. Plots 4a and 4d show the trends of the given parameters, and the Plots 4b and 4c indicate interactions between them. From Plot 4c we see that the impact of dwell time on line width is the same for all step sizes. Thus, no interaction is indicated. However, Plot 4c shows markedly different behavior at the smallest dwell time, revealing that an interaction or nonlinearity exists that has not been accounted for. In Figure 5, we see the trend for the gap width. It should be expected that the gap will shrink in direct proportion to the pitch, but the linear fit of the data (if we concentrate on just the smaller pitches) shows that in fact the gap only shrinks about half as fast as pitch.

Discussion

These results are encouraging. The line and gap widths are the smallest that the authors are aware of for deposition on a bulk surface. The values of the constant term C in the DOE indicate that lines 13–17 nm can be expected and that complementary gap widths 6–10 nm can be comfortably achieved. The process is very stable, and the greatest challenge perhaps is to accurately measure the features because they are so small. Results of similar magnitude have been observed when carrying out the deposition of insulating lines or when doing fine etching. These will be reported at a later time when thorough investigations are completed.

Three items remain outstanding in the present analysis, which should be considered when we look at the low R^2 values obtained; this fit measure became even lower as the pitch of the line pairs was reduced below the 48-nm example shown. Such a poor fit in the analysis indicates that other factors, not captured by the model, are influencing the results. One item is the impact of dwell time on line width, for varying step size, as seen in Figure 4. It sheds some

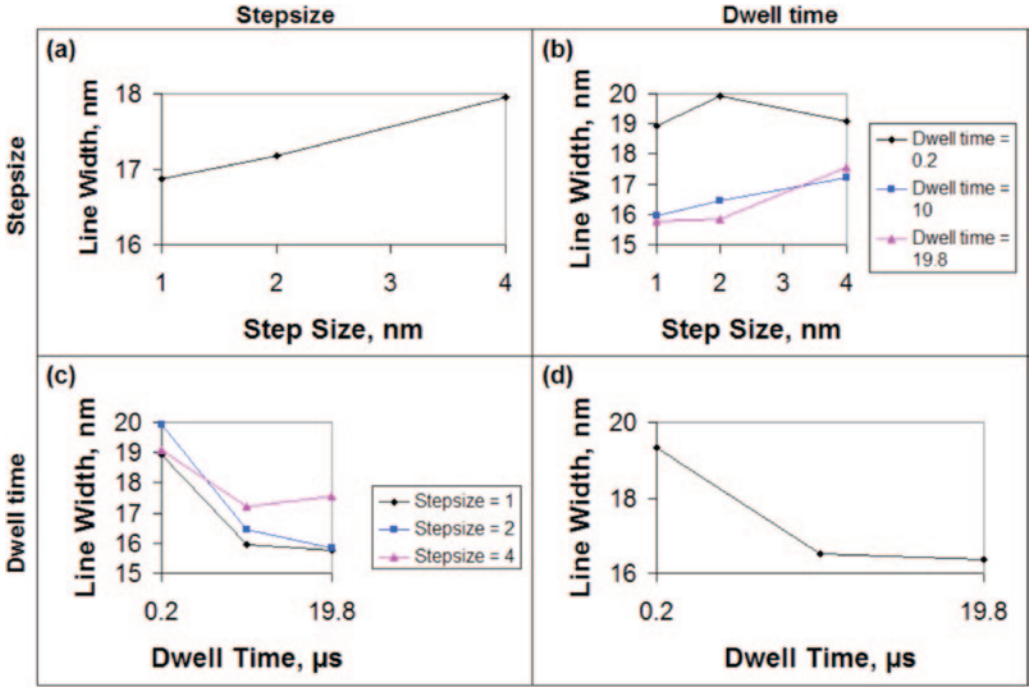

Figure 4: DOE factor analysis plots for the 48-nm pitch pairs. The factors and interaction testing in each matrix element is indicated along the top and left of the matrix of plots (Step Size and Dwell Time). Based on the curves in (a) and (d), it is ascertained that smaller step size and longer dwell time give narrower lines. The family of curves in (b) do not have a uniform trend, indicating that some dependencies probably have not been accounted for. See discussion in the main text.

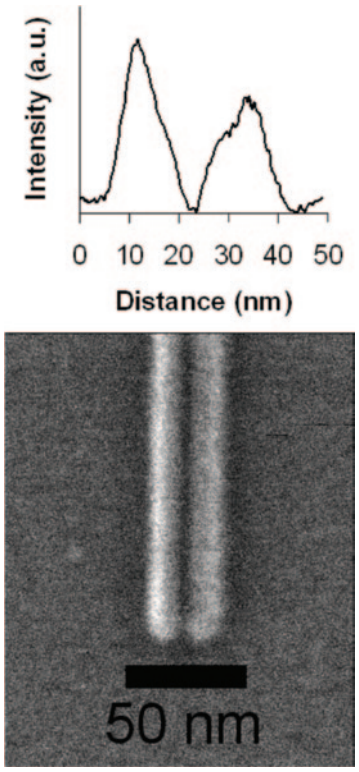

Figure 6: High-magnification image of two lines deposited at 16-nm pitch. A line width of 13-nm is obtained, and even at this small spacing a 6-nm gap is maintained between the lines. The superimposed line scan shows that the lines are asymmetric, possibly due to precursor gas depletion.

light on this situation to realize that the shortest dwell time applied, 0.2 µs, is close to the bandwidth limit of the blanker and scan electronics of the HIM at TNO. Thus, it is not assured that the beam is fully settled into position when jumping from one line to the next. There is also quite an uncharted parameter space between this lowest dwell time and the next one applied, which was 10 µs. Nonlinearity in response might not be captured in this case. It is thought by the authors that a denser sampling of this factor might be in order. The other two items, which are related, have to do with the impact of pitch. The formula for line width does not contain a factor for a nearest-neighbor distance, but Figure 3 clearly indicates that it does matter. Thus, the fit could surely be improved if this were accounted for. The data show a relative insensitivity to this above about 24-nm pitch, so it may show as a non-linear factor, which is of consequence only at the smaller pitch. Related to this is the smaller than expected gap shrinkage. Narrower lines are obtained with small step size and long dwell times—both are factors that deplete more thoroughly the incoming precursor gas feed. Thus, it should not be surprising that when patterning two lines very close to one another that there is gas depletion in the space between the two lines. In fact the best results are obtained under such a condition, as Figure 6 illustrates. From this we measure a line width of just 13 nm and a gap of only 6 nm. It can be observed from the line scan insert in Figure 6 that the deposited material is "pushed" toward the outside of the pairs—at least according to the image gray level. Such a condition will require a more complex model.

Conclusion

The DOE methodology provides the nanoarchitect with a tool to work through the many factors involved in characterizing beam-induced deposition, and it could be extended to other fabrication tasks. The helium ion microscope shows a strong ability in the present case to produce fine features very reproducibly. In fact the main limitation at this point lies with the analysis of the results: line profile measurements by AFM would be a logical next step to get the most accurate measurements. Even then, what if the aspect ratio of the gap becomes large? There are many other factors that confront us, and each will have to be considered as we explore other deposition properties, such as resistivity and compositional purity. A DOE approach assists in the systematic identification of significant factors, which in turn provides valuable hints for improving the instrumentation, recipes, and metrology involved. Making accurate measurements at these length scales will provide interesting challenges for some time to come.

Acknowledgments

The authors would like to acknowledge the many discussions and great technical assistance provided by Mr. Lewis Stern of Carl Zeiss NTS, LLC, during this work.

References

[1] I Utke et al., *J Vac Sci Technol* B 26(4) (2008) 1197.
[2] J Morgan et al., *Microscopy Today* 14(4) (2006) 24–31.
[3] L Scipioni et al., J Vac Sci Technol B 28(6) (2010) C6P18.
[4] PFA Alkemade et al., *Microsc Anal* 24(7) (2010) 5.
[5] D Smith et al., *Nanotechnology* 21 (2010) 175302.
[6] D Montgomery, *Design and Analysis of Experiments*, Wiley, New York, 1991.

MT